Int J Clin Exp Pathol 2020;13(5):1136-1145
www.ijcep.com /ISSN:1936-2625/IJCEP0110276

Original Article

Lin28 is associated with astrocytic proliferation during intracerebral hemorrhage

Wensen Ding[1*], Yuqin Wang[2*], Yaqin Cheng[2], Xin Chen[2], Weiguan Chen[3], Peng Zuo[2], Weihai Chen[4], Zhenguo Qiao[5], Xingjuan Fan[2]

[1]Department of Intensive Care Unit, Affiliated Haian Hospital of Nantong University, Nantong 226600, Jiangsu, China; Departments of [2]Neurology, [3]Rehabilitation Medicine, Affiliated Hospital of Nantong University, Nantong 226001, Jiangsu, China; Departments of [4]Cardiology, [5]Gastroenterology, Suzhou Ninth People's Hospital, Affiliated Wujiang Hospital of Nantong University, Suzhou 215200, Jiangsu, China. [*]Equal contributors.

Received March 4, 2020; Accepted April 14, 2020; Epub May 1, 2020; Published May 15, 2020

Abstract: As an evolutionarily conserved RNA-binding protein, LIN28 is known to be involved in the regulation of the translation and stability of a large number of mRNAs and the biogenesis of certain miRNAs. Increasing evidence indicates that LIN28 regulates many cellular processes, such as embryonic stem cell proliferation, cell fate succession, developmental timing, and oncogenesis. However, the expression and function of LIN28 after intracerebral hemorrhage (ICH) are still unclear. In this study, we performed an intracranial hemorrhage model in adult rats and western blot, immunohistochemistry, as well as immunofluorescence showed that LIN28 was obviously up-regulation in neurons adjacent to the hematoma after ICH. Besides, the transitory increase of LIN28 expression was paralleled with the up-regulation of proliferating cell nuclear antigen (PCNA) as well as GFAP. Hence, LIN28 might play an important role in astrocyte proliferation after ICH.

Keywords: LIN28, intracerebral hemorrhage, astrocytes, proliferation

Introduction

Intracerebral hemorrhage (ICH) is the result of the rupture of cerebral vessels leading to bleeding into the brain parenchyma and/or subarachnoid space [1]. Although ICH contributes to 10-15% of all strokes, it accounts for serious morbidity and mortality worldwide. The 30 day mortality rate is about 35-52%. The 6 month functional independence is only achieved in 20% of the survival individuals [2-4]. The most notable risk factors for ICH are age, hypertension, cerebral amyloid angiopathy, anticoagulants, aneurysms, brain tumours, and so on [5, 6]. Even worse, the incidence of ICH is growing and effective medical and surgical strategies for ICH treatment are still lacking [7, 8]. Therefore, it is essential to develop a better understanding of the potential molecular mechanisms of ICH-induced brain injury. The injury mechanisms during ICH include primary and secondary brain injury. The primary brain injury is due to the formation of hemorrhage and cerebral edema increasing intracranial pressure which leads to brain herniation and blood flow falling (ischaemia). In addition, subsequent rehaemorrhagia and hematoma expansion aggravate the early neurological deterioration. Moreover, the secondary damage takes place through a series of parallel pathological pathways including blood cytotoxicity, excitotoxicity, hypermetabolism, oxidative stress, and inflammation. Ultimately, these mechanisms lead to irreversible disruption of normal tissue structure and neurological function through neuronal apoptosis and necrosis, astrocyte proliferation, and oligodendrocyte death [9-13]. It is to be observed that inflammatory around the clot after ICH is regarded as one of the most important events [12]. However, there still needs researches on the exactly molecular and cellular mechanisms after ICH.

As a heterochronic gene, LIN28 was first identified in the nematode. Caenorhabditiselegans and the expression of LIN28 is stage- and tissue-specific [14]. In mammals,

Lin28 is abundantly expresses in early-stage embryos and upon induction of differentiation the expression is decreasing and restricted in several tissues such as cardiac and skeletal muscles [15]. LIN28 is known to mediate a variety of cellular processes including embryogenesis, skeletal myogenesis, germ cell development, neurogliogenesis, differentiation, lymphopoiesis, and glucose metabolism [16]. As a RNA-binding protein, LIN28 can regulate the translation and stability of a large number of mRNAs and the biogenesis of certain miRNAs. For example, Lin28 can associate with many complexes such as messenger ribonucleoprotein particles (mRNPs), polysomes and stress granules. Besides, LIN28 is involved in regulating cell growth and differentiation in embryonic cells through interacting with let-7 family microRNAs and blocking their processing into mature miRNAs [16-19].

In this study, we found LIN28 was over-expression and colocalization with proliferating cell nuclear antigen (PCNA) during an ICH mode. This study indicates the insight role of LIN28 on the cellular and molecular mechanisms during ICH-induced astrocytes activation.

Materials and methods

Animals and intracerebral infusion

Male Sprague-Dawley rats (240-270 g) provided by the Department of Animal Center, Medical College of Nantong University were used in our study and performed in accordance with National Institutes of Health Guidelines for the Care and Use of Laboratory Animals published by The National Research Council in 1996. Animals were maintained in a 12 h light/dark cycle and at a temperature controlled room (24°C) and animals were divided into a sham group and an experimental group. For ICH model, the animals were deeply anesthetized with 10% chloral hydrate by intraperitoneal injection. 50 μL of autologous whole blood was collected from the tail tip of the animal and injected into the right caudata nucleus stereotactically by use of a microinfusion pump through a 26-gauge needle (coordinates: 0.2 mm anterior, 5.5 mm ventral, and 3.5 mm lateral to the bregma). After infusion for 10 minutes, the needle was kept in situ for over 5 minutes before being withdrawn. The sham group was merely subjected to a needle insertion. The animals were allowed to recover at 37°C room temperature and were provided sufficient food and water after surgery. The animals' brains used for our experiment were removed at an indicated time point after the surgery.

Forelimb placing test

The rats were held by the dorsal torsos in order to make the forelimb hang freely. Independent testing of each forelimb was induced by brushing the vibrissae on the corner edge of a countertop. Intact animals rapidly placed the homolateral forelimb onto the countertop. In the light of the extent of damage, the ICH rats placing of the forelimb contralateral to the injection side indicated it was injured. Each forelimb of every rat was tested 10-15 times and the percentage of placing the left forelimb was recorded.

Corner turn test

The rats were permitted to proceed into a corner with an angle measuring 30°C. In order to exit the corner, the rat must turn either to the right or to the left. Only the turns involving full rearing along either wall was included. According to the extent of damage, the rats may show an inclination to turn to the homolateral side of the injury. The test was conducted 10 times, with an interval between each test at least 30 s. The percentage of right turns was recorded.

Western blot analysis

To get the brain tissue needed for western blotting analysis, the rats were sacrificed at different time points by intraperitoneal injecting chloral hydrate. The brain tissue surrounding the hematoma (extending 2 mm to the hematoma) and the same part of the normal, sham-controlled, and contralateral tissue were dissected and fleetly frozen at -80°C. To obtain brain tissue proteins, the tissues were cut and added to lyses buffer (1% Nonidet P-40, 50 mM Tris, pH 7.5,5 mM EDTA, 1% SDS, 1% sodium deoxycholate, 1% Triton X-100, 1 mM PMSF, 10 lg/mL aprotinin, and 1 lg/mL leupeptin) according to 0.1 g tissue/1 mL lyses buffer. After lysed by the sonifier cell disrupter, the solution was stewed for 40 min, centrifuged at 14,000 rpm for 15 min in a microcentrifuge at 4°C, and collected the superna-

tant. After we measured the concentration with the Bradford assay, the supernatant was subjected to SDS-polyacrylamide gel electrophoresis (PAGE) and transferred to a polyvinylidine difluoride membrane (PVDF) by a transfer apparatus at 300 mA. The membrane was blocked with 5% non-fat milk for 2 h and incubated with primary antibody against LIN28 (anti-rabbit, 1:800; Abcam), PCNA (anti-mouse, 1:800; Santa Cruz), GFAP (anti-mouse, 1:1000; Cell Signaling Technology), and GAPDH (anti-rabbit, 1:1000; Sigma) overnight at 4°C. After washing with PBST for 15 minutes, the membranes were incubated with secondary antibodies for 2 h at room temperature and after washing 45 min, the protein was visualized using an enhanced chemiluminescence system (Pierce Company, USA).

Immunohistochemistry

Rats used for our experiment were anesthetized and perfused with 500 mL of 0.9% saline and 4% paraformaldehyde. After perfusion, the brains were removed and post-fixed in the same fixative for 1 d and the solution was replaced with 20% sucrose for 2 days and then 30% sucrose treatment for 2 days. The brain tissues were embedded in OCT compound to cut 5mm frozen cross-sections. The sections were stored at -20°C. For immunohistochemistry, sections kept at 37°C for 2 h and subjected to 10 mmol/L citrate buffer (pH 6.0) to retrieve the antigen. After washed by 0.01 MPBS for 5 min, the sections were subjected to 3% H_2O_2 for 10 min to reduce endogenous peroxidase activity. After blocked by confining liquid, the sections were incubated with anti-LIN28 antibody (anti-rabbit, 1:100; abcam) for 2 h at 37°C. The sections were washed for 15 min before secondary antibody treatment (Vector Laboratories, Burlingame, CA) for 40 min at 37°C. After stained with DAB (Vector Laboratories), the sections were dehydrated, cleared, and coverslipped after reaction. Slides were examined with a Leica light microscope (Germany) and strong brown staining was regarded as positive and no staining was regarded as negative.

Immunofluorescent staining

For immunofluorescent staining, sections were treated with 1% Triton X-100 for 30 min and blocking solution (10% donkey serum, 1% bovine serum albumin, 0.3% Triton X-100, and 0.15% Tween-20) for 2 h at room temperature. Then, sections were incubated with primary antibodies against LIN28 antibody (anti-rabbit, 1:100; abcam), NeuN (mouse; 1:100; Chemicon), GFAP (mouse; 1:100; Cell Signaling Technology), Iba-1 (mouse; 1:100; Santa Cruz) and PCNA (anti-mouse, 1:100; Santa Cruz) at 4°C overnight. After washed for 15 min, sections were subjected to a mixture of FITC- and CY3-conjugated secondary antibodies at room temperature for 2 h. After washed for 45 min, sections were covered with coverslips. The sections were observed by Leica fluorescence microscope (Wetzlar, Germany).

Quantitative analysis

Cells double labeled for LIN28 and other phenotypic markers were quantified. A minimum of 200 phenotype-specific marker-positive cells surrounding the hematoma were counted in each section to identify the proportion of positive cells. The double labeled cells for LIN28 and phenotype-specific markers were regarded as positive. Three sections consecutive from every rat were sampled.

Cell culture

Primary astrocytes were prepared from the cerebral cortex of newborn Sprague-Dawley rats which were provided by the Department of Animal Center, Medical College of Nantong University. The meaninges were removed carefully to obtain the isolated neopallium which subsequently was cut into 1 mm cubes. After trypsinized by 0.125% [w/v] trypsin for 15 min at 37°C, the tissue suspension was passed through nylon meshes of 70 mm pore size and the cells were seeded at a density of 2×10^9 cells/flask. The cells were cultured with D/F (1:1 DMEM/F12) medium (supplemented with 4-(2-hydroxyethyl)-1-piperazineethanesulfonic acid (HEPES), sodium bicarbonate, and antibiotics) with 10% (v/v) heat-inactivated fetal bovine serum (HI-FBS) at 37°C with a humidified atmosphere of 95% air and 5% CO_2 for 7-10 days. To separate the microglia from the astrocytes, the flasks were placed on a shaker platform and shaken for 8 h at 180 rpm at 37°C. The supernatant was discarded. The medium was changed every 1-2 days. Prior to the experiments, the medium was switched to serum-free DMEM/F12 culture medium.

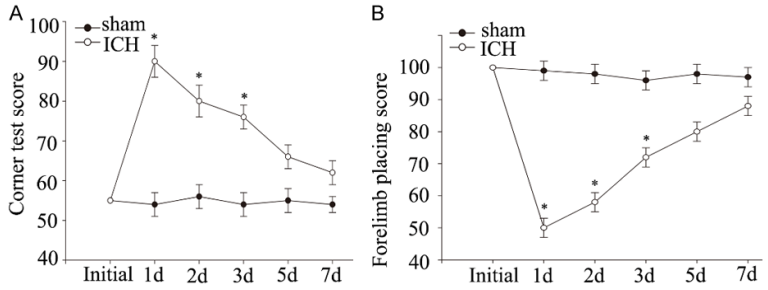

Figure 1. Neurological deficits measured by Behavior Tests after ICH. Corner turn testing (A) and forelimb placing scores (B) at different time points following ICH were performed. The ICH group showed functional deficits compared with the sham-operated group distinctly over the first 3 days (**P*<0.05, significantly different from the sham-operated group), but was with no significant difference at baseline for 7 days later.

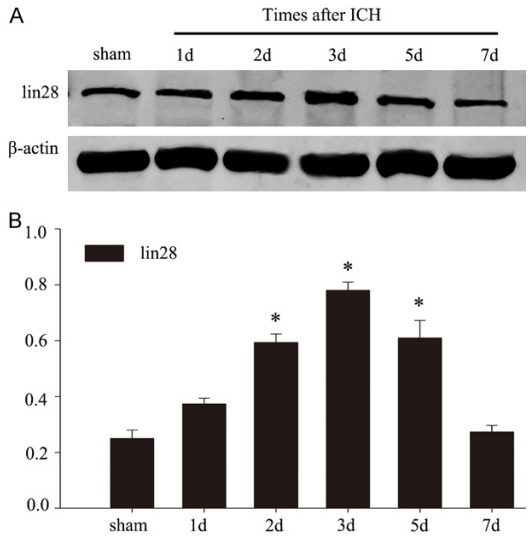

Figure 2. Expression profiles of LIN28 around the hematoma following ICH. A. Western blot was performed to detect the protein levels of LIN28 adjacent to the hematoma at different time points. The expression of LIN28 was relatively low in the sham-operated group, while up-regulated gradually following ICH, peaked at day 3 and declined thereafter. B. The bar graph indicated the density of LIN28 versus β-actin at each time point. Data are presented as mean ± SEM (**P*<0.05).

SiRNA transfection

Primer pairs for the Lin28 siRNA expression vector targeted the sequence of 5'CGGGTAACAGGCCCAGG3'. For transfection, the LIN-28 specific siRNA and nonspecific siRNA vector were transfected using lipofectamine 2000 (Invitrogen) and Plus reagent in basic DMEM (serum free) according to the manufacturer's instructions. After transfection for 36 h, cells were used for western blot.

Statistical analysis

All statistical analyses were conducted with a STATA 7.0 software package (Stata Corp., College Station, TX, USA). All data were expressed as mean ± standard error of mean (S.E.M.). One-way ANOVA was used to compare differences between the treated groups and the control groups. *P*-values <0.05 were considered statistically significant. Each experiment consisted of at least three replicates per condition.

Results

The changes of neurological deficits due to ICH

There are a great number of behavior tests such as corner turn test, forelimb placing test, and rotarod test that was applied to evaluate the alteration of neurological deficits of rats which subjected to an intracranial hemorrhage model [20]. Forelimb placing test and corner turn test were applied to evaluate the functional changes of sensorimotor and plasticity at different time points. The results of the two tests were shown as **Figure 1**, the ICH operation groups exhibited more serious neurological function deficits and the neurological injury was especially obvious within the first 3 d, after which the neurological function recovered gradually.

LIN28 expression is increased after ICH

Western blot was conducted to identify the expression of LIN28 after ICH. As shown in **Figure 2**, the protein level of LIN28 was obviously increased from 1 d and reached the peak at 3 d after ICH (**Figure 2**).

Immunohistochemistry staining of LIN28 around hematoma

To further confirm the protein expression alteration of LIN28 after ICH, immunohistochemistry staining experiment was conducted to compare the expression and distribution of LIN28

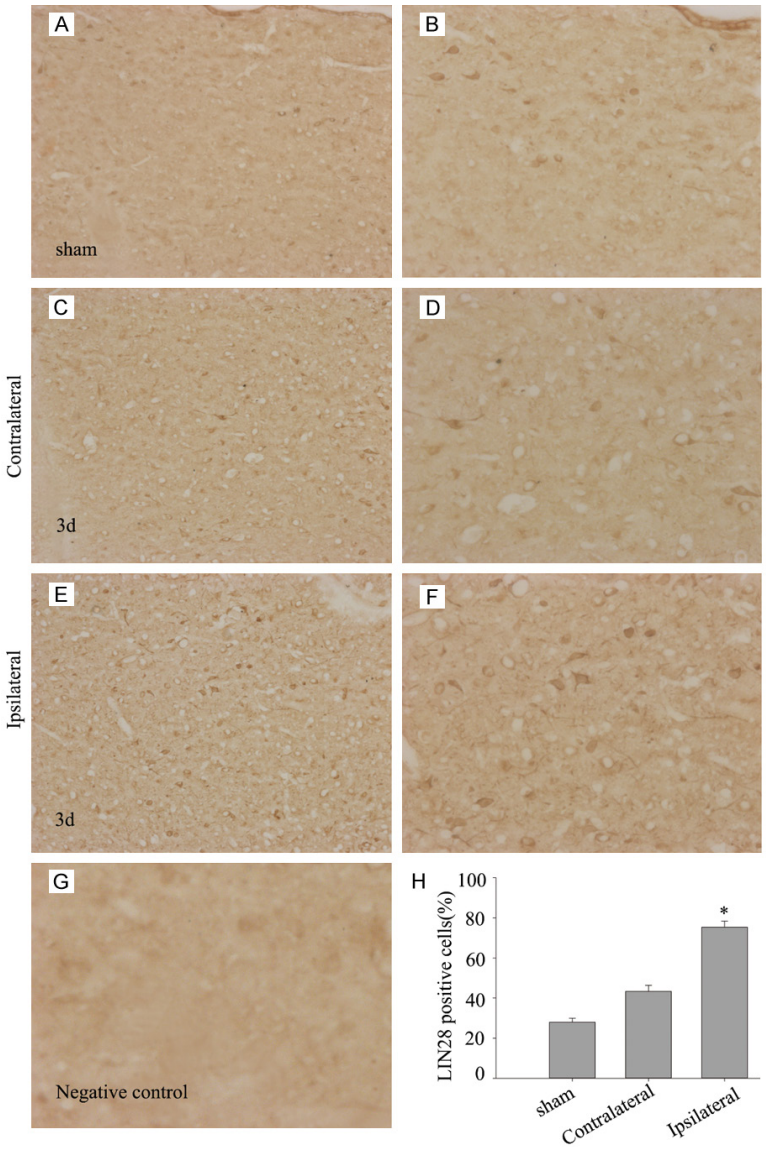

Figure 3. Immunohistochemistry of LIN28 adjacent to the hematoma. Low level of LIN28 signal was found in the sham-operated group (A, B). At 2 days after ICH, the ipsilateral group showed increasing LIN28 signals (E, F), while the contralateral group showed no significant difference in LIN28 compared to sham-operated group (C, D). (G) No positive signal was found in the negative control. (H) The number of LIN28 cells was largely increased comparing the ipsilateral group with the sham-operated and contralateral groups. **P*<0.05 indicated the ipsilateral group was different from the sham-operated and contralateral group with statistical significance. *Scale bar*: left column, 100 μm; right column, 50 μm.

in sham operation and operation group at 2 d. LIN28-positive cells around hematoma after ICH (**Figure 3E**, **3F**) were elevated significantly than the sham (**Figure 3A**, **3B**) and contralateral group (**Figure 3C**, **3D**). Quantitative analysis of LIN28-positive cells around hematoma after ICH was shown as **Figure 3H**. These dates together showed LIN28 was up-regulation after ICH, suggesting that LIN28 played a novel biological function after ICH.

Co-localization of LIN28 with different cellular markers

To further address the role of LIN28, immunofluorescent experiment with different marks (neuron marker NeuN, astrocyte marker GFAP, and microglia marker Iba1) was conducted to determine which cell type LIN28 expressed after ICH. As shown in the **Figure 4**, LIN28 was expressed in both neurons and astrocytes and the co-localization of LIN28 with neurons and astrocytes especially with astrocytes was significantly enhanced surrounding the hemotoma at 3 d after ICH than the sham group.

Association of LIN28 with the cell proliferation

Recently, a study reported that LIN28 was associated with cell proliferation after spinal cord injury [21], so we wondered whether LIN28 interrelate to cell proliferation in rat ICH model. To verify our hypothesis, western blot was conducted to examine the expression level of GFAP and proliferating cell nuclear antigen (PCNA), a general marker of dividing cells surrounding the hematoma in rat brain tissue. As expect, the expression of GFAP and PCNA was enhanced from 1 d and peaked at 5 d after ICH (**Figure 5A**, **5B**). Besides, double-labeling immunofluorescent staining was performed and the result showed that PCNA colocalized with GFAP and LIN28 (**Figure 5C**). This implicated that LIN28 might be associated with cell proliferation after ICH.

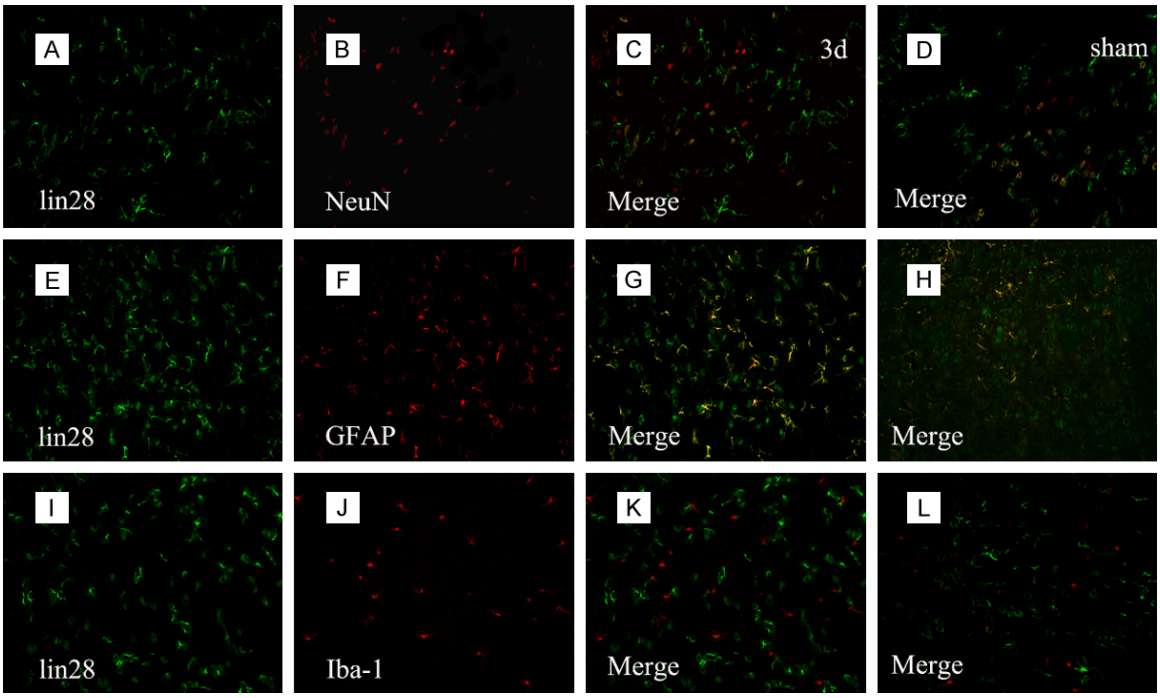

Figure 4. Immunofluorescence staining of LIN28 with different phenotype-specific markers. Sections were labeled with LIN28 (green, A, E, I), neuronal marker NeuN (red, B), astrocyte marker GFAP (red, F) and microglia marker Iba-1 (red, J). The yellow color visualized in the merged images represented the colocalization of LIN28 with different phenotype-specific markers (C, G, K) as well as the sham group (D, H, L). *Scale bars* 50 μm (A-L).

The correlation of LIN28 with the proliferation of astrocytes induced by LPS

As reported, LIN28 was involved in astrocytes inflammation through NF-kB signaling pathway during spinal cord injury [21], so we hypothesized whether LIN28 is involved in astrocytes activation during ICH. Therefore, we used LPS stimulate primary astrocytes which was a typical model of astrocytes activation. Different concentration of LPS was used to stimulating primary astrocytes and western blot was performed to detect the expression of LIN28. As shown in **Figure 6A**, the expression of LIN28 changed along with the dose of LPS and maximum at the concentration of 1 μg/ml. Next, we used 1 μg/ml LPS to stimulate primary astrocytes for different time points. The result indicated that the expression of LIN28 was increased at 12 h and peaked at 18 h. The expression of PCNA and astrocyte-specific glial fibrillary acidic protein (GFAP) were also increased at 12 h and peaked at 18 h and 24 h (**Figure 6C**). The parallel expression of LIN28 with PCNA and GFAP implied LIN28 was associated with astrocytes activation. To further confirm the role of LIN28, primary astrocytes were transfected with LIN28 specific, non-specific siRNA and vehicle. Western blot was performed to examine LIN28 expression after transfected for 48 h, and LIN28 specific-siRNA obviously down-regulated LIN28 expression (**Figure 6E**). After being transfected for 30 h, primary astrocytes were then subjected to LPS treatment for another 18 h and western blot was performed to test the expression of LIN28, PCNA, and GFAP. The result showed that the expression of LIN28, PCNA, and GFAP were reduced after LIN28 knocked down and LPS stimulation (**Figure 6G**). Based on the above experiments, we have sufficient reasons to draw the conclusion that LIN28 was involved on astrocyte proliferation.

Discussion

The injury mechanisms of ICH include physical trauma and mass effect, cerebral blood flow reduction, thrombin, erythrocytes, haemoglobin, iron, inflammation, and complement [10, 22]. The inflammatory response surrounding the haematoma involves enzyme activation, mediator release, inflammatory cell migration, glial activation, brain tissue breakdown and

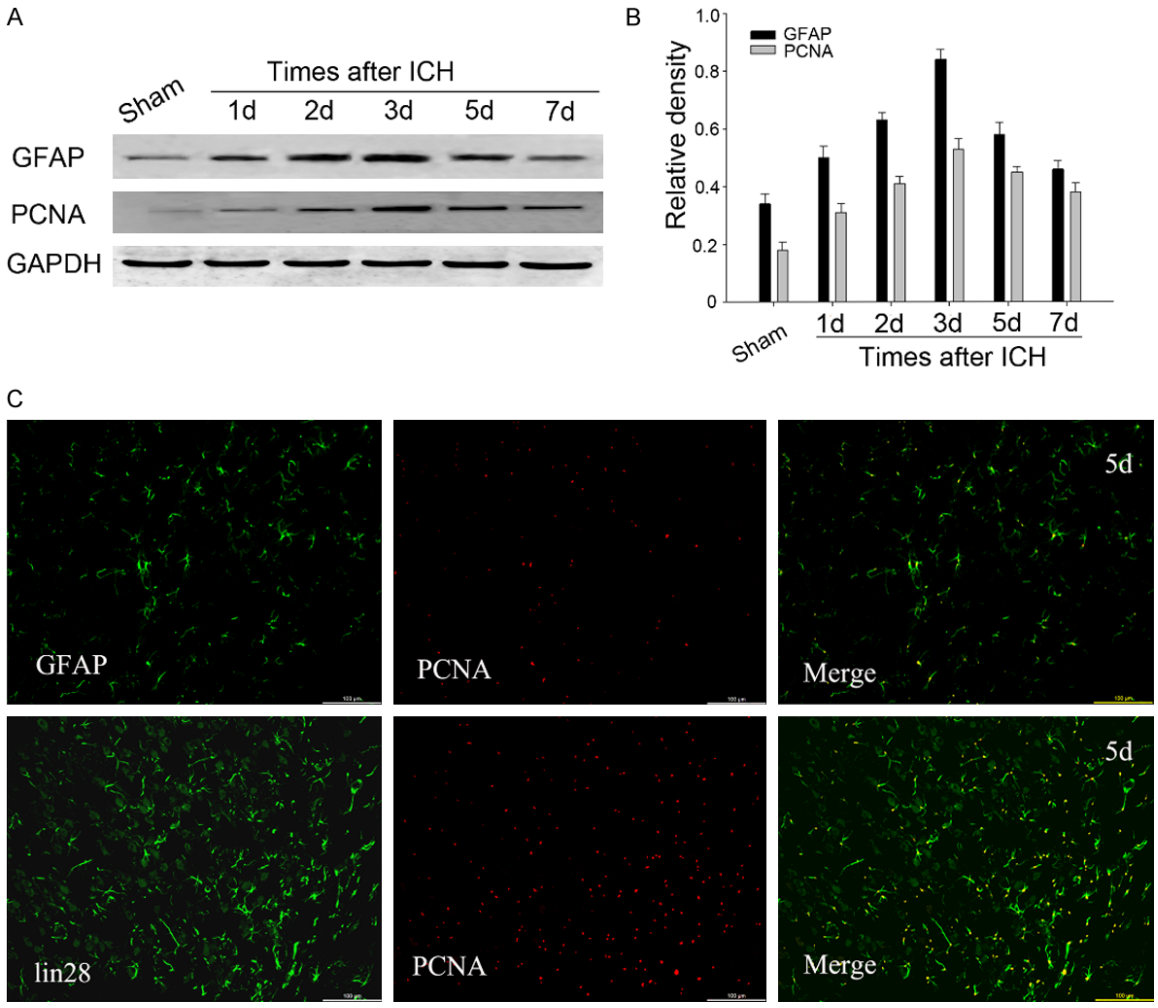

Figure 5. Correlations of LIN28 with astrocyte proliferation following ICH. (A) Western blot analysis showed the expression of GFAP and PCNA increased and peaked at day 3. (B) The bar graph indicated the density of GFAP and PCNA versus GAPDH at each time point. Data are presented as mean ± SEM ($^{*,\#}P<0.05$). Double immunofluorescent staining showed the colocalization of PCNA/GFAP and LIN28/PCNA in brain basal ganglia adjacent to the hematoma at 3 days after ICH (C). *Scale bars* 50 μm (C).

repair, which aggravate haemorrhagic brain injury in turn [23, 24]. As the predominant glial cell type in the central nervous system (CNS), astrocytes play critical functions in maintaining ionic hemostasis, metabolizing toxins, regulating scar tissue, preventing neovascularization, supporting synaptogenesis and neurogenesis as well as innate immune response [25-27]. In addition, astrocytes play significant roles on neurons. For example, astrocytes can modulate neuronal survival after ICH by regulating neuronal resistant to oxidative stress [28], as well as affect neuronal injury by modulating brain inflammation [29]. Thus, astrocyte-mediated inflammatory response plays an important role in the pathogenesis of brain injuries after ICH. Many studies showed that astrocytes undergo proliferation, phenotypic changes, and cellular hypertrophy after brain injuries induced by traumatic or ischemic brain insults [30, 31]. Therefore, developing a better understanding of the molecular and cellular mechanisms of astrocytes activation caused by ICH-induced inflammation is necessary.

Our present study revealed that LIN28 was transiently up-expression surrounding the hematoma and peaked at 3 d after ICH. Immunofluorescent staining revealed that LIN28 was mainly colocalization with neurons and astrocytes. In addition, the enhanced expression of LIN28 was paralleled with the increase of GFAP and PCNA which implied the up-regulation of LIN28 might be involved in astro-

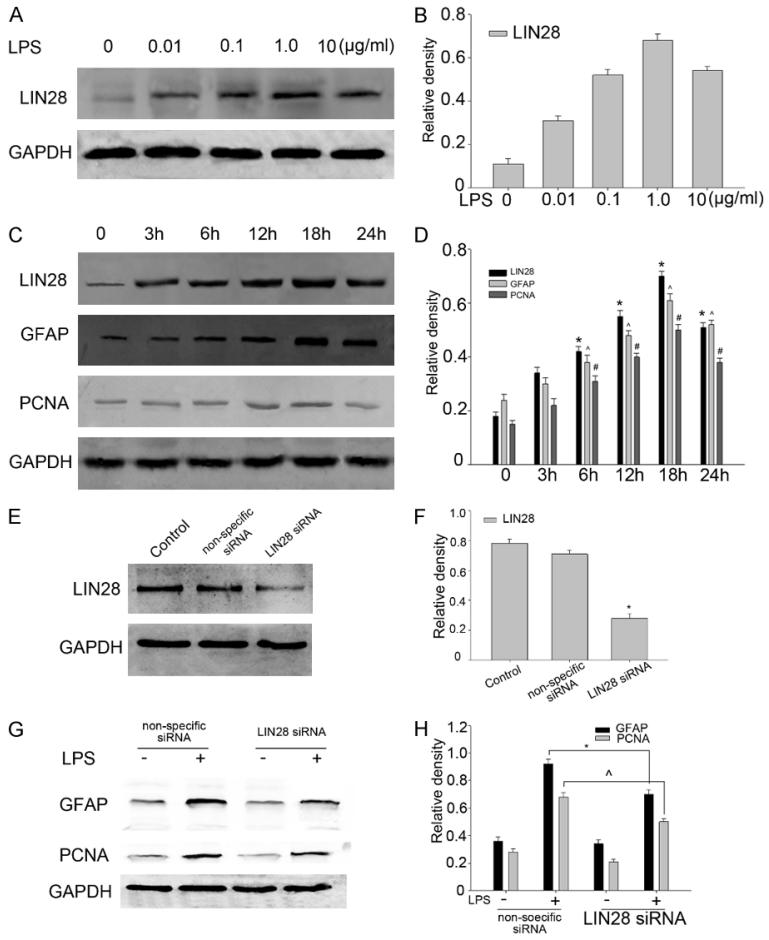

Figure 6. HERPUD1 modulated cell proliferation in vitro. Primary cultured astrocytes stimulated with different concentration of LPS, and LIN28 expression maxed at the concentration of 1 μg/ml (A, B). We used 1 μg/ml LPS to stimulate primary astrocytes at different time points. The expression of LIN28 was increased at 12 h and peaked at 18 h. The expression of PCNA and GFAP were also increased at 12 h and peaked at 18 h (C, D). Western blot analysis showed siRNA silenced LIN28 in primary cultured astrocytes (E, F). The knockdown of LIN28 induced down-regulated levels of PCNA and GFAP expression (G). The bar graph indicated the relative density of LIN28, PCNA and GFAP versus GAPDH (H). Data are mean ± SD, n=3, $P<0.05$.

cytes activation after ICH-induced inflammation. To further verify our hypothesis, we used the LPS stimulation to induce astrocytes activation model in vitro and the results showed that the expression of LIN28 was parallel with the expression of the two proteins. We applied the siRNA of LIN28 to knock down the expression of LIN28 in primary astrocytes which subjected to LPS stimulation for 18 h. The results showed that eliminated LIN28 expression could weaken LPS-induced GFAP and PCNA expression. Thus we have sufficient proof to hypothesis that LIN28 might play an important role in astrocytes activation after ICH.

The animal ICH model used in our experiment deserves to be mentioned. The most commonly used ICH model was intracerebral injection of collagenase to cause vessel rupture or direct injection of blood into the brain [10, 32]. The two models have advantages and self deficits. The collagenase-induced haemorrhage is due to disrupt vasculature, but widespread dissolution of the endothelial basement membrane might cause disruption of several blood vessels, which is different from the spontaneous ICH. In addition, the collagenase has toxic impacts on brain parenchymal cells. However, the intraparenchymal blood injection mimics the effects of an intracerebral haematoma but it lacks the ruptured blood vessels which is the primary cause of ICH [9, 10, 32]. Therefore, relevant models of spontaneous ICH in animals are greatly needed.

In summary, our current study might provide an innovative way to illustrate the underlying molecular and cellular mechanisms following ICH-induced astrocytes activation and LIN28 might represent a potentially molecular target for the treatment of ICH. However, much deeper researches are still needed on the exact role of LIN28 on astrocytes activation.

Acknowledgements

This work was supported by the Nantong science and technology project (HS2014033).

Disclosure of conflict of interest

None.

Address correspondence to: Dr. Zhenguo Qiao, Department of Gastroenterology, Suzhou Ninth

People's Hospital, 2666 Ludang Road, Suzhou 215200, Jiangsu Province, China. Tel: +86-0512-82881198; E-mail: qzg66666666@163.com; Dr. Xingjuan Fan, Department of Neurology, Affiliated Hospital of Nantong University, 20 Xisi Road, Nantong 226001, Jiangsu Province, China. Tel: +86-0513-85052222; E-mail: ntfanxj@163.com

References

[1] Feigin VL, Lawes CM, Bennett DA, Barker-Collo SL and Parag V. Worldwide stroke incidence and early case fatality reported in 56 population-based studies: a systematic review. Lancet Neurol 2009; 8: 355-69.

[2] van Asch CJ, Luitse MJ, Rinkel GJ, van der Tweel I, Algra A and Klijn CJ. Incidence, case fatality, and functional outcome of intracerebral haemorrhage over time, according to age, sex, and ethnic origin: a systematic review and meta-analysis. Lancet Neurol 2010; 9: 167-76.

[3] LoPresti MA, Bruce SS, Camacho E, Kunchala S, Dubois BG, Bruce E, Appelboom G and Connolly ES. Hematoma volume as the major determinant of outcomes after intracerebral hemorrhage. J Neurol Sci 2014; 345: 3-7.

[4] Kuramatsu JB, Huttner HB and Schwab S. Advances in the management of intracerebral hemorrhage. J Neural Transm (Vienna) 2013; 120 Suppl 1: S35-41.

[5] Ariesen MJ, Claus SP, Rinkel GJ and Algra A. Risk factors for intracerebral hemorrhage in the general population: a systematic review. Stroke 2003; 34: 2060-5.

[6] Jackson CA and Sudlow CL. Is hypertension a more frequent risk factor for deep than for lobar supratentorial intracerebral haemorrhage? J Neurol Neurosurg Psychiatry 2006; 77: 1244-52.

[7] Söderholm M, Inghammar M, Hedblad B, Egesten A and Engström G. Incidence of stroke and stroke subtypes in chronic obstructive pulmonary disease. Eur J Epidemiol 2016; 31: 159-68.

[8] Wilson D, Charidimou A and Werring DJ. Advances in understanding spontaneous intracerebral hemorrhage: insights from neuroimaging. Expert Rev Neurother 2014; 14: 661-78.

[9] Keep RF, Hua Y and Xi G. Intracerebral haemorrhage: mechanisms of injury and therapeutic targets. Lancet Neurol 2012; 11: 720-31.

[10] Xi G, Keep RF and Hoff JT. Mechanisms of brain injury after intracerebral haemorrhage. Lancet Neurol 2006; 5: 53-63.

[11] Qureshi AI, Mendelow AD and Hanley DF. Intracerebral haemorrhage. Lancet 2009; 373: 1632-44.

[12] Aronowski J and Zhao X. Molecular pathophysiology of cerebral hemorrhage: secondary brain injury. Stroke 2011; 42: 1781-6.

[13] Gong C, Boulis N, Qian J, Turner DE, Hoff JT and Keep RF. Intracerebral hemorrhage-induced neuronal death. Neurosurgery 2001; 48: 875-82.

[14] Moss EG, Lee RC and Ambros V. The cold shock domain protein LIN-28 controls developmental timing in C. elegans and is regulated by the lin-4 RNA. Cell 1997; 88: 637-46.

[15] Yang DH and Moss EG. Temporally regulated expression of Lin-28 in diverse tissues of the developing mouse. Gene Expr Patterns 2003; 3: 719-26.

[16] Li N, Zhong X, Lin X, Guo J, Zou L, Tanyi JL, Shao Z, Liang S, Wang LP, Hwang WT, Katsaros D, Montone K, Zhao X and Zhang L. Lin-28 homologue A (LIN28A) promotes cell cycle progression via regulation of cyclin-dependent kinase 2 (CDK2), cyclin D1 (CCND1), and cell division cycle 25 homolog A (CDC25A) expression in cancer. J Biol Chem 2012; 287: 17386-97.

[17] Xu B, Zhang K and Huang Y. Lin28 modulates cell growth and associates with a subset of cell cycle regulator mRNAs in mouse embryonic stem cells. RNA 2009; 15: 357-61.

[18] Balzer E and Moss EG. Localization of the developmental timing regulator Lin28 to mRNP complexes, p-bodies and stress granules. RNA Biol 2007; 4: 16-25.

[19] Viswanathan SR and Daley GQ. Lin28: a microRNA regulator with a macro role. Cell 2010; 140: 445-9.

[20] Okauchi M, Hua Y, Keep RF, Morgenstern LB and Xi G. Effects of deferoxamine on intracerebral hemorrhage-induced brain injury in aged rats. Stroke 2009; 40: 1858-63.

[21] Yue Y, Zhang D, Jiang S, Li A, Guo A, Wu X, Xia X, Cheng H, Tao T and Gu X. LIN28 expression in rat spinal cord after injury. Neurochem Res 2014; 39: 862-74.

[22] Xue M and Del Bigio MR. Intracerebral injection of autologous whole blood in rats: time course of inflammation and cell death. Neurosci Lett 2000; 283: 230-2.

[23] Wang X and Lo EH. Triggers and mediators of hemorrhagic transformation in cerebral ischemia. Mol Neurobiol 2003; 28: 229-44.

[24] Wang J and Doré S. Inflammation after intracerebral hemorrhage. J Cereb Blood Flow Metab 2007; 27: 894-908.

[25] Panickar KS and Norenberg MD. Astrocytes in cerebral ischemic injury: morphological and general considerations. Glia 2005; 50: 287-98.

[26] Eddleston M and Mucke L. Molecular profile of reactive astrocytes--implications for their role in neurologic disease. Neuroscience 1993; 54: 15-36.

[27] Dong Y and Benveniste EN. Immune function of astrocytes. Glia 2001; 36: 180-90.

[28] Swanson RA, Ying W and Kauppinen TM. Astrocyte influences on ischemic neuronal death. Curr Mol Med 2004; 4: 193-205.
[29] Pyo H, Yang MS, Jou I and Joe EH. Wortmannin enhances lipopolysaccharide-induced inducible nitric oxide synthase expression in microglia in the presence of astrocytes in rats. Neurosci Lett 2003; 346: 141-4.
[30] Ridet JL, Malhotra SK, Privat A and Gage FH. Reactive astrocytes: cellular and molecular cues to biological function. Trends Neurosci 1997; 20: 570-7.
[31] Liu L, Rudin M and Kozlova EN. Glial cell proliferation in the spinal cord after dorsal rhizotomy or sciatic nerve transection in the adult rat. Exp Brain Res 2000; 131: 64-73.
[32] Rosenberg GA, Mun-Bryce S, Wesley M and Kornfeld M. Collagenase-induced intracerebral hemorrhage in rats. Stroke 1990; 21: 801-7.